Video Article

Hollow Microneedle-based Sensor for Multiplexed Transdermal Electrochemical Sensing

Philip R. Miller[1,2], Shelby A. Skoog[1], Thayne L. Edwards[2], David R. Wheeler[2], Xiaoyin Xiao[2], Susan M. Brozik[2], Ronen Polsky[2], Roger J. Narayan[1]

[1]Joint Department of Biomedical Engineering, University of North Carolina and North Carolina State University

[2]Department of Biosensors and Nanomaterials, Sandia National Laboratories

Correspondence to: Ronen Polsky at rpolsky@sandia.gov, Roger J. Narayan at roger_narayan@unc.edu

URL: https://www.jove.com/video/4067
DOI: doi:10.3791/4067

Keywords: Bioengineering, Issue 64, Biomedical Engineering, Microneedle, Microneedle sensors, multiplexed detection, electrochemistry, stereolithography

Date Published: 6/1/2012

Citation: Miller, P.R., Skoog, S.A., Edwards, T.L., Wheeler, D.R., Xiao, X., Brozik, S.M., Polsky, R., Narayan, R.J. Hollow Microneedle-based Sensor for Multiplexed Transdermal Electrochemical Sensing. *J. Vis. Exp.* (64), e4067, doi:10.3791/4067 (2012).

Abstract

The development of a minimally invasive multiplexed monitoring system for rapid analysis of biologically-relevant molecules could offer individuals suffering from chronic medical conditions facile assessment of their immediate physiological state. Furthermore, it could serve as a research tool for analysis of complex, multifactorial medical conditions. In order for such a multianalyte sensor to be realized, it must be minimally invasive, sampling of interstitial fluid must occur without pain or harm to the user, and analysis must be rapid as well as selective.

Initially developed for pain-free drug delivery, microneedles have been used to deliver vaccines and pharmacologic agents (e.g., insulin) through the skin.[1-2] Since these devices access the interstitial space, microneedles that are integrated with microelectrodes can be used as transdermal electrochemical sensors. Selective detection of glucose, glutamate, lactate, hydrogen peroxide, and ascorbic acid has been demonstrated using integrated microneedle-electrode devices with carbon fibers, modified carbon pastes, and platinum-coated polymer microneedles serving as transducing elements.[3-7,8]

This microneedle sensor technology has enabled a novel and sophisticated analytical approach for in situ and simultaneous detection of multiple analytes. Multiplexing offers the possibility of monitoring complex microenvironments, which are otherwise difficult to characterize in a rapid and minimally invasive manner. For example, this technology could be utilized for simultaneous monitoring of extracellular levels of, glucose, lactate and pH,[9] which are important metabolic indicators of disease states[7,10-14] (e.g., cancer proliferation) and exercise-induced acidosis.[15]

Video Link

The video component of this article can be found at https://www.jove.com/video/4067/

Protocol

1. Microneedle Fabrication

1. Using three-dimensional modeling software Solidworks (Dassault Systemes SA, Velizy, France), design a pyramidal-shaped hollow microneedle array (**Figure 1**).[3-5]
2. Design a support structure for the microneedle array using Magics RP 13 software (Materialise NV, Leuven, Belgium). The support structure allows the resin to drain from the device during fabrication and provides a base on which the microneedles are built. An example support structure is shown in **Figure 1**.
3. The linked support and microneedle array files are uploaded into the Perfactory RP software (EnvisionTEC GmbH, Gladbeck, Germany), which controls the fabrication process. Within this software package, choose the number of microneedle arrays to be fabricated and determine the placement of devices on the fabrication plate.
4. Run calibration in ultraviolet mode at 180 mW for the Perfactory rapid prototyping manufacturing system and verify the deviation in energy is within ±2 mW.
5. Once fabrication is complete, remove the microneedle arrays from the baseplate and develop in isopropanol for 15 minutes. Dry the arrays with compressed air and cure the microneedles at room temperature for 50 seconds in the Otoflash Postcuring System (EnvisionTEC GmbH, Gladbeck, Germany) to ensure complete polymerization.
6. Validate microneedle fabrication via microscopy and verify that each microneedle bore is hollow and unobstructed. Fully-fabricated microneedles are shown in **Figure 2**.

2. Fabrication of Carbon Paste Electrode Arrays

1. Use a 60 W Model 6.75 CO_2 raster/vector laser system (Universal Laser Systems, Inc., Scottsdale, AZ) to cut holes and expose the underlying individually addressable connecting copper wires in a flat flexible cable (21039-0249), which was obtained from a commercial source (Molex Connector Corp., Lisle, IL) (**Figure 3 (A and B)**). Place the flat flexible cables in a jig to properly align them on the laser ablation plate. Use a rastering approach to create 500 µm diameter cavities in the insulating portion of the flexible cable. Patterns for ablation are created in CorelDraw (Corel, Ottawa, Ontario) and sent to the laser system.
2. Clean the modified flat flexible cables with an airbrush that sprays acetone at 40 psi. Finish cleaning them by rinsing with isopropanol and deionized water. Verify under a microscope that no insulating film remains over the exposed copper strips.
3. The next step is to create a holding cavity for packing of carbon pastes. Melinex tape (0.002" thickness coated on a single side with pressure sensitive acrylic adhesive) is ablated with the same pattern as the electrode strips, oriented over the ablated electrode strips, and compressed at 3000 psi for 2 minutes to ensure a proper connection. In this case, the cavity diameter is 750 µm.
4. An additional layer of Melinex tape (0.004" thickness coated on two sides with pressure sensitive acrylic adhesive) is subsequently ablated in the same pattern as the single-sided adhesive tape and is used after alignment to bond the microneedle arrays to the carbon paste electrode arrays.

3. Synthesis of Functional Carbon Pastes and Packing of Electrode Cavities

1. The glucose sensitive carbon paste is based off of a previous recipe and is obtained by mixing 10 mg of glucose oxidase and 2.2 mg of poly(ethylenimine) until a homogeneous mixture is obtained.[16] To this mixture, 60 mg of rhodium on carbon powder (5% loading) is added. 40 mg mineral oil is added and subsequently mixed. The pastes are stored at 4 °C until use; the pastes are used up to one week after preparation.
2. The pH sensitive carbon paste is obtained by mixing 30% (w/w) mineral oil and 70% (w/w) graphite powder. Pack paste into the electrode cavity as described in section 3.4. Make solution of 10 mM Fast Blue RR diazonium salt (4-benzoylamino-2,5-dimethoxybenzenediazonium chloride hemi (zinc chloride) salt) in 0.5 M phosphoric acid.[17], Place a 20 µl drop of this solution over the packed paste electrode for 30 minutes to spontaneously chemisorb the Fast Blue PR diazonium salt. Rinse with deionized water and store in buffer or deionized water when not in use.
3. The lactate sensitive carbon paste is based off of a previous recipe and is obtained by mixing 2.5 mg of rhodium on carbon powder and 2.5 mg of lactate oxidase, alternating between 5 minutes of sonication and 5 minutes of vortexing for five rotations.[18]
4. Packing of the modified pastes into the prepared flat flexible cable is accomplished by applying the respective pastes over the electrode cavities. Using a thin piece of plastic (e.g., an edge of a plastic weigh boat) as a trowel and pack the paste until a smooth surface is achieved. Repeat with a second clean weighing boat until excess paste is removed. Wash with deionized water. A schematic showing laser ablation to create cavities, packing of carbon pastes, and microneedle integration (described in section 2 and 3) is presented in **Figure 3**.

4. Detection and sensor calibration

1. Lactate detection is accomplished by measuring the chronoamperometric response of the sensor at -0.15 V and recording the current after 15 seconds in 0.1 M phosphate buffer (pH=7.5). **Figure 4(a)** contains a schematic of the electrocatalytic reaction for detection of lactate.
2. Glucose detection is performed in a similar manner by measuring the chronoamperometric response of the sensor at -0.05 V and recording the current after 15 seconds in 0.1 M phosphate buffer (pH 7.0). **Figure 4(b)** contains a schematic of the electrocatalytic reaction for detection of glucose.
3. pH is monitored by running cyclic voltammetric scans from -0.7 V to 0.8 V at 100 mV/s and recording the position of the oxidative peak potential. A schematic of the redox reactions for pH detection is shown in **Figure 5**.
4. Calibration curves for glucose and lactate sensors can be created by successive additions of the respective analyte; chronoamperometric measurements are performing after each analyte addition as described in sections 5.1 and 5.2. Alternatively, fixed potential chronoamperometric measurements can be made under stirring while allowing sufficient time (~10-100 seconds) in between each analyte addition for current stabilization.
5. pH calibration curves can be created by measuring the position of the oxidative peak potential over a series of known pH values from 5 to 8 in 1.0 pH unit increments and recording cyclic voltammograms as described in section 5.3.

5. Representative Results

When obtaining chronoamperometric curves (e.g., for glucose detection or lactate detection) in quiescent solutions with modified carbon paste-filled microneedles, the current will immediately decrease upon application of the respective detection potential. It will eventually decay to a steady state value. A representative result is shown in **Figure 6**; this result was obtained from 2 mM additions of lactate and recording at the lactate microneedle. The solution must be briefly stirred after each lactate addition. The current after 15 seconds rises upon increasing the concentration of lactate; the current response can then be used to determine the concentration of lactate in an unknown solution. Alternatively, continuous monitoring can be used in a stirred solution (or in a flowing solution) as demonstrated for a solution with an increasing glucose concentration (**Figure 5**). Again, the increase in current upon increasing the concentration of glucose can be used to standardize the glucose response to an unknown solution. Sufficient time must be allowed after each spike in order to allow the solution to stabilize. Cyclic voltammograms at the pH sensitive microneedle in 0.1 M phosphate buffer are shown over four different pH solutions from 5 to 8 in 1 pH unit increments in **Figure 6**. The oxidative peak potential shifts with increasing pH; this phenomenon is used as an indicator of the pH value.

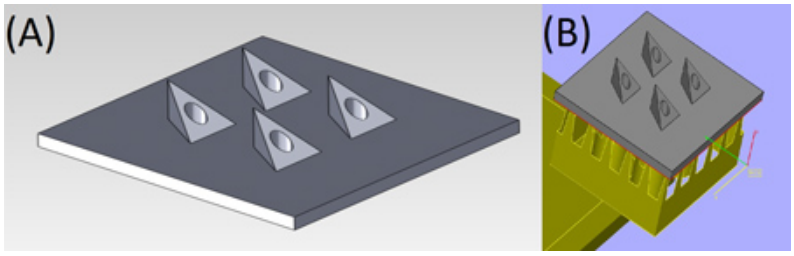

Figure 1. Images of the STL file of the microneedle array created in Solidworks (A) and of the print screen, which shows the support structure (B).

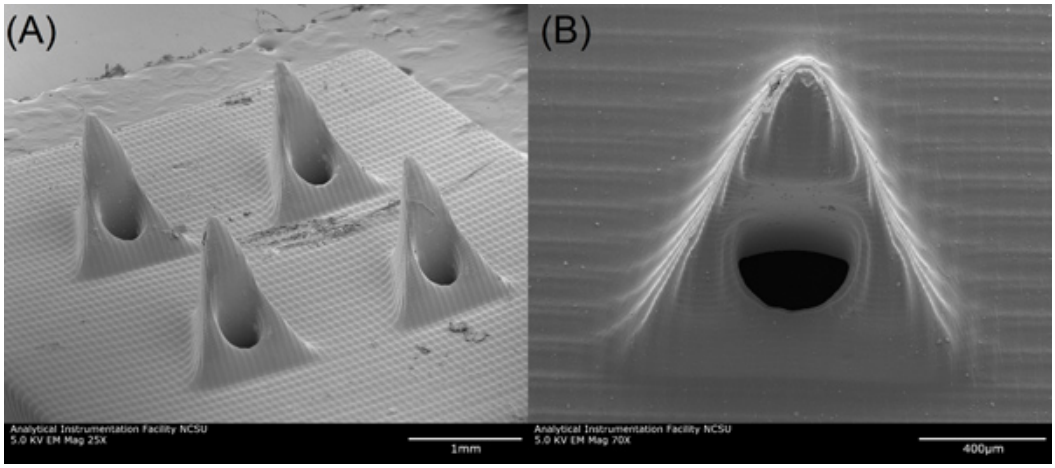

Figure 2. Scanning electron micrographs of the microneedle array (A) and a single microneedle within this array (B).

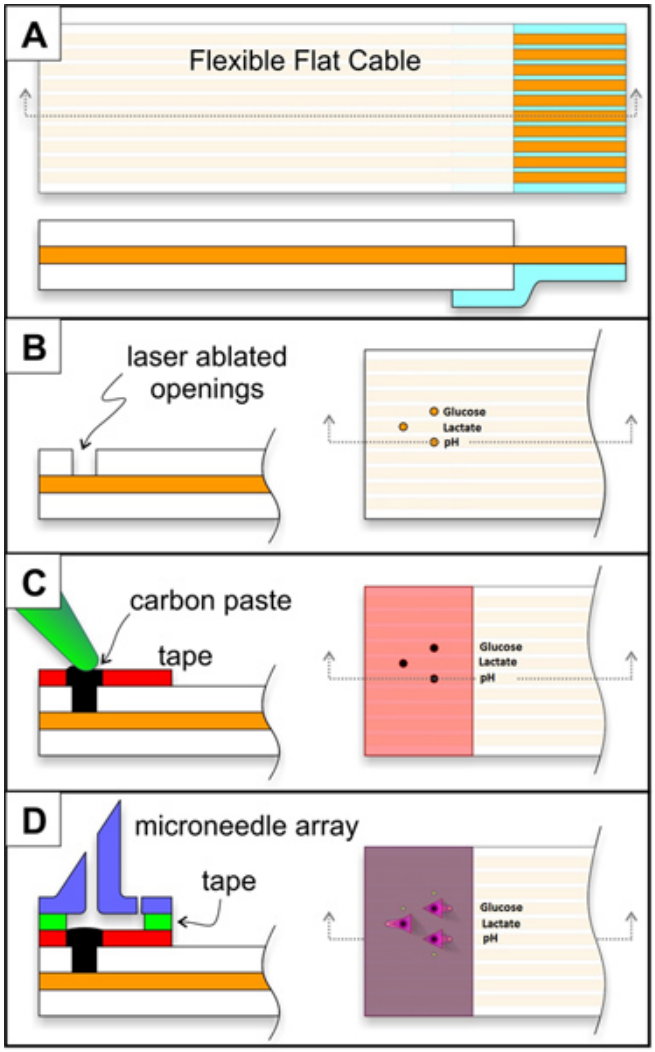

Figure 3. Schematic of flat flexible cable assembly. The steps involved include modifying the flat flexible cable (A), ablating the patterned circles (B), adding the initially ablated Melinex layer, which is filled with carbon paste (C), as well as adding the second ablated Melinex layer and mating the microneedle array (D). Click here to view larger figure.

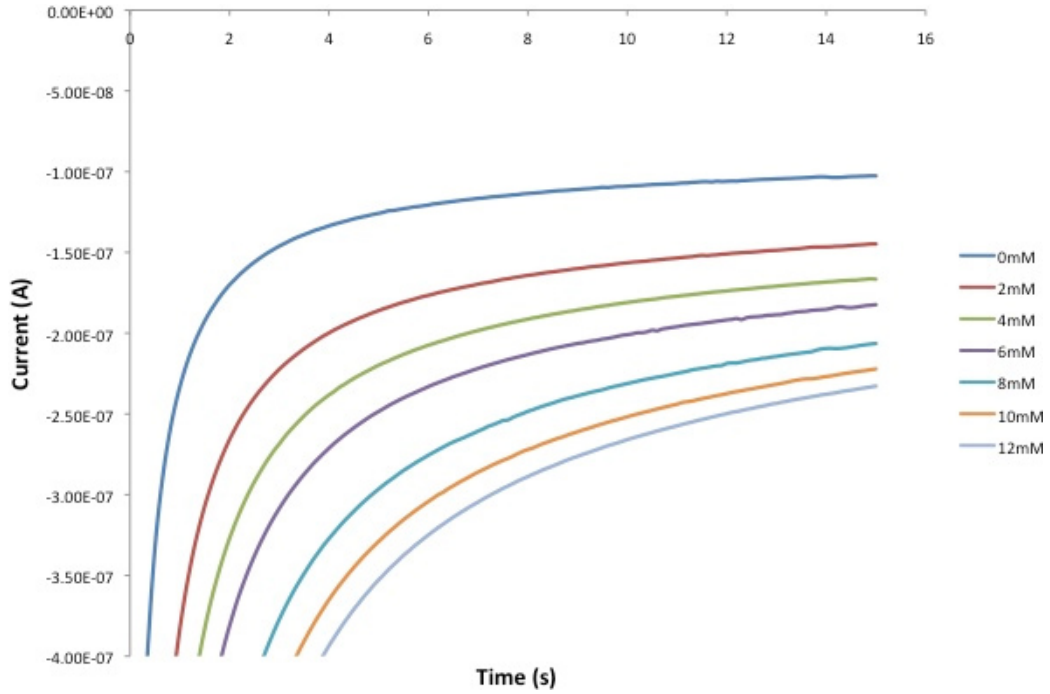

Figure 4. Calibration of lactate-sensitive paste with 15 second chronoamperometric scans at -0.15 V in 0.1 M phosphate buffer (pH=7.5). Each increase in current corresponds to a 2 mM addition of lactate.

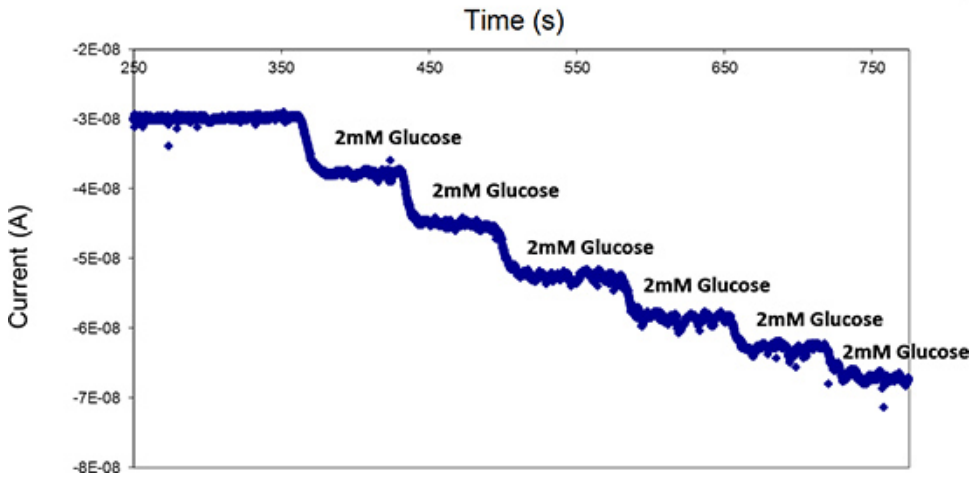

Figure 5. Calibration of glucose-sensitive paste running chronoamperometric scans at -0.05 V. Each decrease in the response corresponds to a 2 mM addition of glucose. The 0.1 M phosphate buffer solution (pH=7.0) was stirred during calibration. External Ag/AgCl and Pt reference and counter electrodes were used in this study.

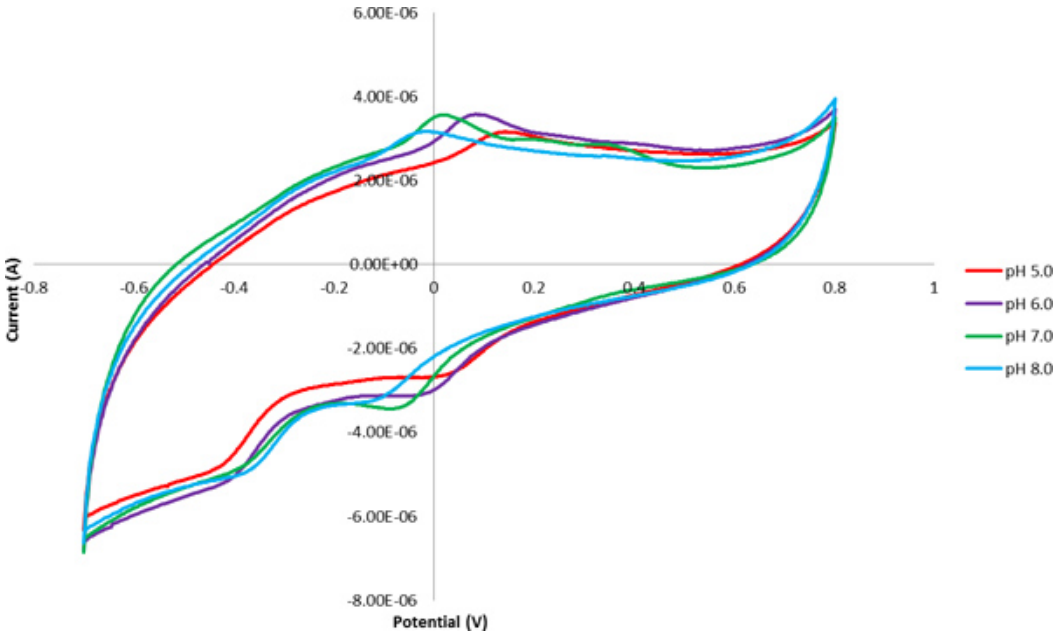

Figure 6. Cyclic voltammogram (CV) of pH sensitive carbon paste in 0.1 M phosphate buffer over pH 5-8 in 1 pH unit increments (teal=pH 8.0, green=pH 7.0, purple=pH 6.0, red=pH 5.0). A fifth CV was used for analysis versus Ag/AgCl reference and Pt wire counter electrodes.

Discussion

Multiple aspects of the design of this microneedle-based sensor were considered prior to device fabrication. In order to use this sensor for real-time detection, the response time of the sensor must be low; in this protocol, each tested sensor exhibited a response time below fifteen seconds. Pastes used in this protocol were also chosen for their selectivity within *in vivo* environments, which contain electroactive biomolecules that can interfere with electrode response. In addition to paste composition, the operating potentials were chosen to minimize the influence of interfering electroactive species. Successful fabrication of the microneedle array involves the selection of a suitable microneedle design and microneedle material. These two aspects will determine if the microneedle can puncture the skin, protect the electrodes from physical damage, and preclude electrode-tissue contact. It should be noted that an external Ag/AgCl and Pt reference and counter electrodes were used during measurements; in vivo use of this device with human or animal subjects would require that these electrodes be incorporated within the device.

Each component of the microneedle-based sensor has features that must be validated to ensure proper functionality. Quality control during modification of the flat flexible cable (**Figure 3 B**) involves ensuring that the insulating layer is completely removed from the surface of the tin-plated copper wires after laser ablation (**Figure 3**). Failure to remove the insulating layer from the surface of the copper wire after laser ablation can cause irregular responses due to incomplete electrical contact. The laser-ablated Melinex tape needs to be examined with a microscope to ensure that the diameter of each opening is consistent as it defines the working area of the electrode. When applying carbon paste to the laser-ablated Melinex tape cavities, the paste must conform to the exact hole diameter with no excess in order to avoid signal variations due to differences in surface area. During chronoamperometric measurements with modified carbon pastes, the signal must stabilize to a limiting value before current is recorded. These results can slightly vary due to mixing effects. Mechanical testing of the microneedle arrays was performed prior to sensor incorporation; in a previous study, our group showed these arrays were capable of puncturing porcine skin, which was used as an analog for human skin.[3] Microneedle arrays should not undergo deformation or fracture during skin penetration since these processes could lead to electrode damage.

This protocol has detailed the construction of a novel transdermal device for electrochemical monitoring. We envision future efforts involving microneedle sensors with an even greater number of individually addressable microneedles and a greater variety of transducers. This device was designed for analysis of interstitial fluid in humans; use with animals is also possible with appropriate species-specific modifications to microneedle design. Future directions with this technology include but are not limited to remote patient monitoring as well as coupling with a drug delivery device for automated sensing-drug delivery.

Disclosures

No conflicts of interest declared.

Acknowledgements

Sandia is multiprogram laboratory operated by Sandia Corporation, a Lockheed Martin Company, for the United Stated Department of Energy's National Nuclear Security Administration under Contract DE-AC04-94AL85000. The authors acknowledge funding from Sandia National Laboratories' Laboratory Directed Research & Development (LDRD) program.

References

1. Henry, S., McAllister, D.V., Allen, M.G., & Prausnitz, M.R. Microfabricated microneedles: a novel approach to transdermal drug delivery. *J. Pharm. Sci.* **87**, 922-925 (1998).
2. Prausnitz, M.R. Microneedles for transdermal drug delivery. *Adv. Drug Deliv. Rev.* **56**, 581-587 (2004).
3. Miller, P.R., Gittard, S.D., Edwards, T.L., Lopez, D.M., Xiao, X., Wheeler, D.R., Monteiro-Riviere, N.A., Brozik, S.M., Polsky, R., & Narayan, R.J. Integrated carbon fiber electrodes within hollow polymer microneedles for transdermal electrochemical sensing. *Biomicrofluidics.* **5**, 013415 (2011).
4. Windmiller, J.R., Zhou, N., Chuang, M.C., Valdés-Ramírez, G., Santhosh, P., Miller, P.R., Narayan, R., & Wang, J. Microneedle array-based carbon paste amperometric sensors and biosensors. *Analyst.* **136**, 1846-1851 (2011).
5. Windmiller, J.R., Valdés-Ramírez, G., Zhou, N., Zhou, M., Miller, P.R., Jin, C., Brozik, S.M., Polsky, R., Katz, E., Narayan, R., & Wang, J. Bicomponent microneedle array biosensor for minimally-invasive glutamate monitoring. *Electroanal.* **23**, 2302-2309 (2011).
6. Ricci, F., Moscone, D., & Palleschi, G. *Ex vivo* continuous glucose monitoringwith microdalysis technique: The example of GlucoDay. *IEEE Sensors J.* **8**, 63-70 (2008).
7. Zimmermann, S., Fienbork, D., Flounders, A.W., & Liepmann, D. In-device enzyme immobilization: Wafer-level fabrication of an integrated glucose sensor. *Sens. Actuat. B.* **99**, 163-173 (2004).
8. Miller, P.R., Skoog, S.A., Edwards, T.L., Lopez, D.M., Wheeler, D.R., Arango, D.C., Xiao, X., Brozik, S.M., Wang, J., Polsky, R., & Narayan, R.J. Multiplexed microneedle-based biosensor array for characterization of metabolic acidosis. *Biomicrofluidics.* **88**, 739-742 (2012).
9. Miller, P.R., Skoog, S.A., Edwards, T.L., Lopez, D.M., Wheeler, D.R., Arango, D.C., Xiao, X., Brozik, S.M., Wang, J., Polsky, R., & Narayan, R.J. Multiplexed microneedle-based biosensor array for characterization of metabolic acidosis. *Talanta.* **88**, 739-742 (2012).
10. Rofstad, E.K. Microenvironment-induced cancer metastasis. *Int. J. Radiat. Biol.* **76**, 589-605 (2000).
11. Vander Heiden, M.G., Cantley, L.C., & Thompson, C.B. Understanding the Warburg effect: the metabolic requirements of cell proliferation. *Science*. **324**, 1029-1033 (2009).
12. Warburg, O., Wind, F., & Negelein, E. The metabolism of tumors in the body. *J. Gen. Physiol.* **8**, 519-530 (1927).
13. Goode, J.A. & Chadwick, D.J., Eds. *The Tumour Microenvironment: Causes and Consequences of Hypoxia and Acidity.* Novartis Foundation Symposium 240, John Wiley & Sons, Ltd., (2008).
14. Cardone, R.A., Casavola, V., & Reshkin, S.J. The role of disturbed pH dynamics and the Na+/H+ exchanger in metastasis. *Nature Rev. Cancer.* **5**, 786-795 (2005).
15. Robergs, R.A., Ghiasvand, F., & Parker, D. Biochemistry of exercise-induced metabolic acidosis. *Am. J. Phys.* **287**, R502-R516 (2004).
16. Wang, J., Liu, J., Chen, L., & Lu, F. Highly selective membrane-free, mediator-free glucose biosensor. *Anal. Chem.* **66**, 3600-3603 (1994).
17. Makos, M.A., Omiatek, D.M., Ewing, A.G., & Heien, M. L. Development and characterization of a voltammetric carbon-fiber microelectrode pH sensor. *Langmuir.* **26**, 10386-10391 (2010).
18. Wang, J., Chen, Q., & Pedrero, M. Highly selective biosensing of lactate at lactate oxidase containing rhodium-dispersed carbon paste electrodes. *Anal. Chem. Acta.* **304**, 41-46 (1995).

